ARTICLE IN PRESS

+ MODEL

Available online at www.sciencedirect.com

SCIENCE DIRECT®

ELSEVIER

Progress in Solid State Chemistry xx (2005) 1–6

Progress in Solid State Chemistry

www.elsevier.com/locate/pssc

Structural and magnetic properties of thin manganite films grown on silicon substrates

I. Bergenti [a,*], V. Dediu [a], E. Arisi [a], M. Cavallini [a], J.F. Moulin [a], F. Biscarini [a], M. De Jong [b], C. Dennis [c], J. Gregg [c]

[a] *ISMN CNR, via P. Gobetti 101, 40129 Bologna, Italy*
[b] *Department of Physics, IFM, Linköping University, S-581 83 Linköping, Sweden*
[c] *Clarendon Laboratory, University of Oxford, Parks Road, Oxford OX1 3PU, UK*

Abstract

Polycrystalline $La_{0.7}Sr_{0.3}MnO_3$ manganite thin films were grown on silicon substrates covered by SiO_x amorphous native oxide. Unusual splitting of the manganite layer was found: on the top of an intermediate layer characterised by lower crystalline order, a magnetic robust layer is formed. Curie temperatures of about 325 K were achieved for 70 nm thick films. A strong room temperature XMCD signal was detected indicating high spin polarisation near the surface.

1. Introduction

Spin-dependent electric transport is widely investigated nowadays due to the possibility of building a new class of electronic devices which operate based on spin as the memory element (spintronics) [1]. In this framework, silicon (Si) has a potential application due to its long spin coherence time [2].

The spin injection process from a ferromagnetic reservoir at the interface to Si or any other semiconducting materials (SC) is mainly controlled by the conductivity mismatch limitations [3]. A consistent spin injection can be obtained either by using ferromagnetic semiconductors (FS) [4] or by using complex metallic oxides. Good spin injection has been achieved using FS as for example (Ga,Mn)As but their application is limited by the Curie temperatures still well

* Corresponding author.
E-mail address: i.bergenti@bo.ismn.cnr.it (I. Bergenti).

0079-6786/$ - see front matter © 2005 Elsevier Ltd. All rights reserved.
doi:10.1016/j.progsolidstchem.2005.11.004

below room temperature. Among the ferromagnetic oxides, colossal magnetoresistive half metal oxide of composition $La_{0.7}Sr_{0.3}MnO_3$ (LSMO) is a good candidate for spin injection given its low carrier density (10^{21}–10^{22} cm^{-3}), high spin polarisation of charge carriers and room temperature ferromagnetism ($T_C = 370$ K) [5]. The development of hybrid LSMO-Si based spintronic devices requires good control of the magnetic properties and spin polarisation of the LSMO thin films deposited on Si. While epitaxial LSMO thin films can be grown on single-crystal oxide substrates with lattice-matching parameters, as for example $SrTiO_3$ (STO), reports of LSMO thin films grown on silicon substrates are very limited in the literature. Epitaxial LSMO thin films on Si have been mainly obtained by using buffer layer as STO and YSZ [6,7] while polycrystalline films have been grown directly on the substrate or on amorphous SiO_x [8].

The two cases are obviously characterised by different manganite–substrate interface properties. For understanding and controlling these interfaces the development of reliable technologies able to provide high quality ferromagnetic films in both polycrystalline and epitaxial phase is required. In this article we investigate the spin polarisation properties and the crystalline structure of polycrystalline LSMO film grown on Si/SiO_x.

2. Experiment

LSMO films were grown by pulsed plasma deposition (PPD) [9] under an oxygen pressure of about 2×10^{-2} mbar. In this technique, the ablation process is due to a pulsed electron beam, generated by an electron avalanche process, hitting on a stoichiometric target. Most of the ablated material escapes in the form of molten nanodroplets or cluster with the conservation of the stoichiometry in deposited films. Thin films were grown on silicon (100) substrates with a native 2 nm thick SiO_2 top layer. Two substrate temperatures were considered: 680 °C and 740 °C. All the samples were annealed in situ in a vacuum at 400 °C. The sample thickness was measured by the conventional alfa step technique.

The high resolution electron microscopy (HREM) and analysis were performed at 300 kV on a JEOL JEM-3000F FEGTEM. The images were acquired digitally onto a Gatan model 794 (1k × 1k) CCD camera. Electron energy loss imaging (EELI) and spectroscopy (EELS) experiments were performed with a Gatan imaging filter (GIF), equipped with a 2k 794IF/20 MegaScan CCD camera. Data were acquired using part of the spectrum to reform the image of the sample. This technique can be used to select energy losses corresponding to particular chemical elements or states (compositional mapping). Energy dispersive X-ray spectroscopy (EDS) was performed on an Oxford Instruments EDS with a super atmospheric thin window (SATW) detector.

A comprehensive microstructural analysis has been carried out using scanning electron microscopy (SEM; Hitachi S4000) and atomic force microscopy (SMENA NT-MDT Moscow).

The magnetic properties were investigated by means of the magneto-optical Kerr effect (MOKE). MOKE was detected in the longitudinal configuration with an He–Ne laser ($\lambda = 632.8$ nm, $P = 5$ mW). The polarised laser light was focused on the surface of the sample placed in a sweeping external magnet field. Variation of the polarisation of the reflected light depending on the magnetisation of the sample was detected as a function of the temperature.

X-Ray magnetic circular dichroism (XMCD) measurements were performed at beamline D1011 of the MAX-II storage ring, located at the MAX-Laboratory for Synchrotron Radiation Research in Lund, Sweden. The angle of incidence of the photon beam was set to 60° relative to the sample normal. The in-plane magnetisation of the LSMO films was set by applying

a magnetic field pulse of about 200 G. The XMCD spectra were recorded with a fixed helicity of the light and opposite magnetisation directions [10].

3. Results and discussion

For all the investigated samples, X-ray diffraction spectra (Fig. 1) are characteristic for the rhombohedral phase. The films are not textured indicating a polycrystalline structure. By indexing the LSMO peaks with pseudocubic indexes a lattice parameter of 3.84 ± 0.02 Å is obtained. The existence of other structural phases (orthorhombic, tetragonal or monoclinic) cannot be excluded a priori from these measurement due to the relatively weak intensity of the diffraction peaks.

The cross sectional TEM analysis shows two distinct layers formed in the LSMO as shown in Fig. 2. The contrast should be the result of one region being more dense than the other; consequently the darker region has a higher crystalline order as seen by the enlarged image (Fig. 2b). The lattice parameters deduced from the FFT of the HREM image are in good agreement with those associated with the rhombohedral LSMO structure ($a = 3.8 \pm 0.2$ Å). The elemental analysis shows that the LSMO layer is compositionally homogeneous and in spite of the high deposition temperature there is no evidence for diffusion of Si into the LSMO layer most likely prevented by the SiO_x layer. On the other hand, some local oxygen diffusion into the Si through the SiO_x barrier has been observed. Moreover, no signature of chemical reaction at the interface has been found and the SiO_x layer remains quite distinct throughout. We ought to exclude a temperature driven transition from a layer with very low spatial correlation to a polycrystalline layer. Most likely the crystalline order of the transition LSMO layer is mainly due to minor local compositional variations, i.e. O, La and/or Sr inhomogeneity. This is confirmed by AFM measurements indicating that the morphology of the analysed films is not dependent on deposition temperature. The same AFM measurements indicate that the film surface is composed of grains with a mean diameter size of 100 nm (Fig. 3a). SEM micrography confirms this result as seen in Fig. 3b.

The magnetic properties of the surface and then of the upper crystalline LSMO layer were investigated by both MOKE and XMCD. Fig. 4 shows the XMCD curve at $T = 130$ K and $T = 300$ K obtained by taking the difference of X-ray absorption spectroscopy spectra at the

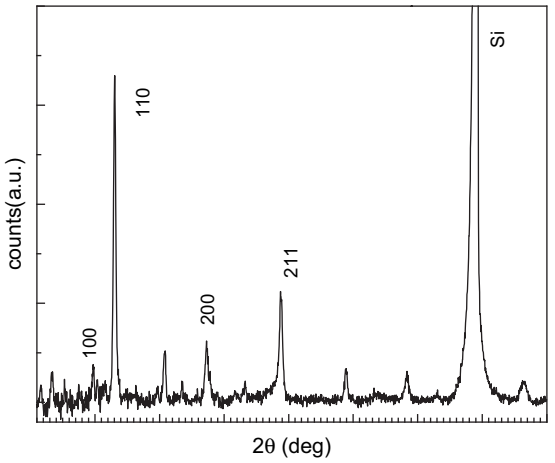

Fig. 1. X-Ray diffraction pattern for 70 nm thick thin film deposited at 680 °C.

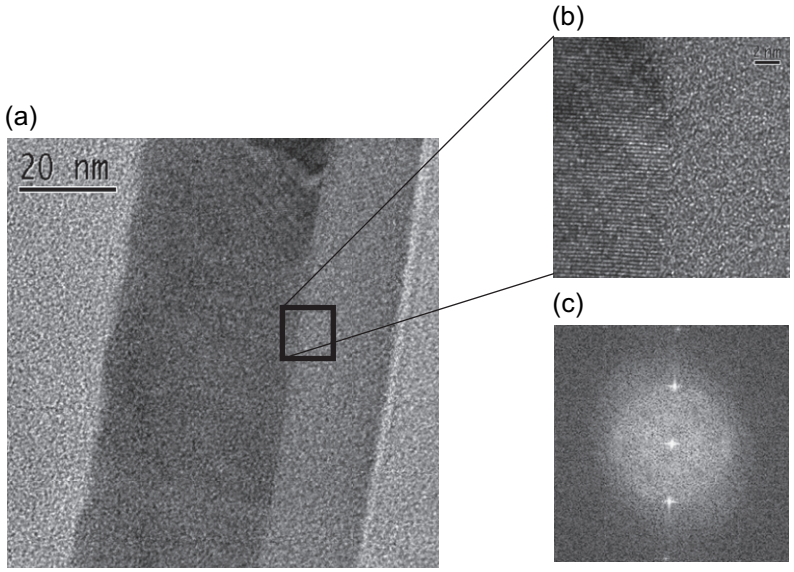

Fig. 2. HRTEM image of a cross-section of LSMO deposited at 680 °C. (a) HREM image taken at a magnification of 200k× (scale bar shown on image). The very dark and medium grey sections of the image are the LSMO, with the epoxy glue on the left and the Si on the right. The white line at the junction between the Si and the medium grey region is the SiO_2 layer. The dark region has significantly more crystalline areas than the medium grey region. (b) HREM image taken at a magnification of 1000k× (scale bar shown on image) to examine the interface between the two LSMO layers. (c) FFT of the image shows the crystalline structure.

$L_{2,3}$ edge Mn energy with in-plane magnetisation parallel and anti-parallel to the helicity of the circularly polarised light for the sample deposited at 680 °C. The angle of incidence of the primary beam allowed us to investigate the ferromagnetism up to 3 nm from the surface. The LSMO at the surface is clearly ferromagnetic with an XMCD curve similar to those of epitaxial LSMO films [5]. At room temperature, the XMCD signal is still present and, to the best of our knowledge, this is the first experimental result of room temperature spin polarisation in manganite deposited on silicon.

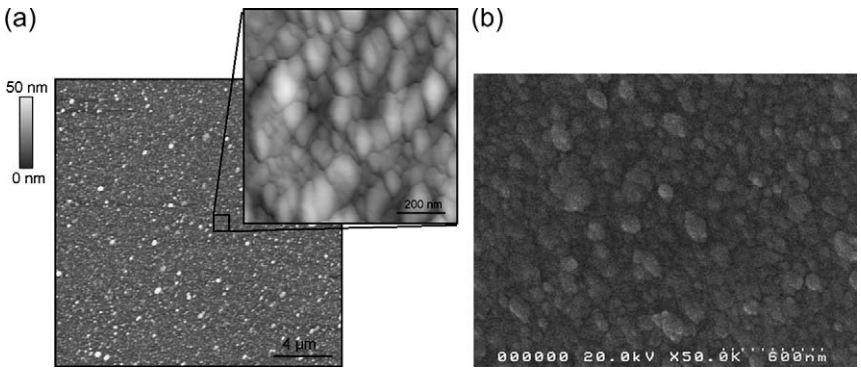

Fig. 3. (a) AFM topographic images of LSMO film grown at 740 °C. The granular structure of the sample becomes clear at higher magnifications. (b) SEM image collected at 20 kV shows the granular structure. Bar scale on the image.

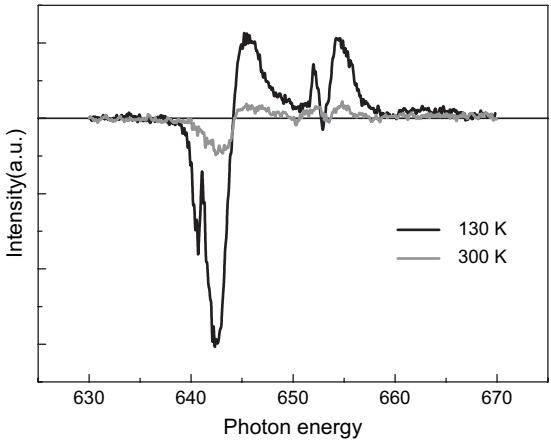

Fig. 4. The XMCD curves of LSMO deposited at 680 °C collected at $T = 130$ K (black line) and 300 K (grey line). The curves were normalised to the integrated Mn $L_{2,3}$ edge XAS intensity.

The MOKE signal for all the investigated samples shows a hysteretic loop. The temperature dependence of the MOKE signal for two substrate temperatures is shown in Fig. 5. The onset of ferromagnetism is established above room temperature and the deduced Curie temperatures are 325 K and 310 K respectively. Effect of morphology and disorder at the grain boundaries should be responsible for the different loop shapes.

The magnetic nature and the role in spin injection of the LSMO intermediate layer is still unclear. Measurements of AC susceptibility indicate that only one ferromagnetic transition is present. This is consistent with an LSMO layer characterised by short range correlated grains without any substantial magnetic transition.

4. Conclusions

LSMO thin films with high ferromagnetic order at room temperature have been deposited directly on Si substrates covered by native SiO_x without any additional buffer layer. The

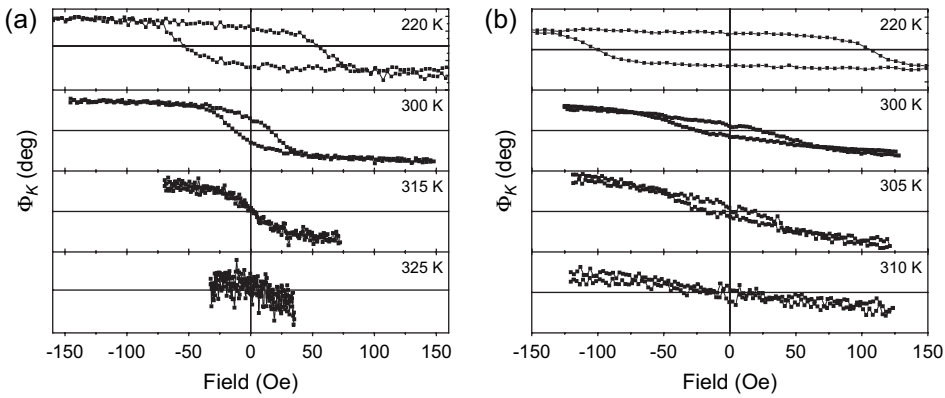

Fig. 5. Longitudinal Kerr rotation measured for 70 nm thick film deposited at 680 °C(a) and 740 °C (b) collected at different temperatures.

amorphous SiO_x layer induces the formation of a manganite intermediate layer of a few nanometers characterised by lower crystallographic order over which polycrystalline growth takes place. The remarkable surface ferromagnetic properties found at room temperature without any additional buffer layer makes them very interesting as a spin source in silicon based technology.

References

[1] Das Sarma S. Am Sci 2001;89:516.
[2] Gordon JP, Bowers KD. Phys Rev Lett 1958;1:368.
[3] Schmidt G, Ferrand D, Molenkamp LW, Filip AT, van Wees BJ. Phys Rev B 2000;62:R4790.
[4] Matsukura F, Ohno H, Shen A, Sugawara Y. Phys Rev B 1998;57:R2037.
[5] Park J-H, Vescovo E, Kim H-J, Kwon C, Ramesh R, Venkatesan T. Phys Rev Lett 1998;81:1953.
[6] Pradhan AK, Mohanty S, Kai Zhang, Dadson JB, Jackson EM, Hunter D, et al. Appl Phys Lett 2005;86:012503.
[7] Kim J-H, Khartsev SI, Grishin AM. Appl Phys Lett 2003;82:4295.
[8] Dubourdieu C, Audier M, Sénateur JP, Pierre J. J Appl Phys 1999;86:6945.
[9] Dediu VI, Jiang QD, Matacotta FC, Scardi P, Lazzarino M, Nieva G, et al. Supercond Sci Technol 1995;8:160.
[10] Stohr J. NEXFAS spectroscopy. Berlin: Springer-Verlag; 1996.